View metadata, citation and similar papers at core.ac.uk

brought to you by CORE

provided by Crossref

Hindawi Publishing Corporation
Journal of Thermodynamics
Volume 2013, Article ID 169674, 9 pages
http://dx.doi.org/10.1155/2013/169674

Research Article

MHD Stagnation-Point Flow of Casson Fluid and Heat Transfer over a Stretching Sheet with Thermal Radiation

Krishnendu Bhattacharyya

Department of Mathematics, The University of Burdwan, Burdwan, West Bengal 713104, India

Correspondence should be addressed to Krishnendu Bhattacharyya; krish.math@yahoo.com

Received 28 May 2013; Accepted 3 September 2013

Academic Editor: Felix Sharipov

Copyright © 2013 Krishnendu Bhattacharyya. This is an open access article distributed under the Creative Commons Attribution License, which permits unrestricted use, distribution, and reproduction in any medium, provided the original work is properly cited.

The two-dimensional magnetohydrodynamic (MHD) stagnation-point flow of electrically conducting non-Newtonian Casson fluid and heat transfer towards a stretching sheet have been considered. The effect of thermal radiation is also investigated. Implementing similarity transformations, the governing momentum, and energy equations are transformed to self-similar nonlinear ODEs and numerical computations are performed to solve those. The investigation reveals many important aspects of flow and heat transfer. If velocity ratio parameter (B) and magnetic parameter (M) increase, then the velocity boundary layer thickness becomes thinner. On the other hand, for Casson fluid it is found that the velocity boundary layer thickness is larger compared to that of Newtonian fluid. The magnitude of wall skin-friction coefficient reduces with Casson parameter (β). The velocity ratio parameter, Casson parameter, and magnetic parameter also have major effects on temperature distribution. The heat transfer rate is enhanced with increasing values of velocity ratio parameter. The rate of heat transfer is enhanced with increasing magnetic parameter M for $B > 1$ and it decreases with M for $B < 1$. Moreover, the presence of thermal radiation reduces temperature and thermal boundary layer thickness.

1. Introduction

In fluid dynamics the effects of external magnetic field on magnetohydrodynamic (MHD) flow over a stretching sheet are very important due to its applications in many engineering problems, such as glass manufacturing, geophysics, paper production, and purification of crude oil. The flow due to stretching of a flat surface was first investigated by Crane [1]. Pavlov [2] studied the effect of external magnetic field on the MHD flow over a stretching sheet. Andersson [3] discussed the MHD flow of viscous fluid on a stretching sheet and Mukhopadhyay et al. [4] presented the MHD flow and heat transfer over a stretching sheet with variable fluid viscosity. On the other hand, Fang and Zhang [5] reported the exact solution of MHD flow due to a shrinking sheet with wall mass suction. Bhattacharyya and Layek [6] showed the behavior of solute distribution in MHD boundary layer flow past a stretching sheet. Furthermore, many vital properties of MHD flow over stretching sheet were explored in various articles [7–12] in the literature. Several important investigations on the flow due to stretching/shrinking sheet are available in the literature [13–16].

Chiam [17] investigated the stagnation-point flow towards a stretching sheet with the stretching velocity of the plate being equal to the straining velocity of the stagnation-point flow and found no boundary layer structure near the sheet. Mahapatra and Gupta [18] reconsidered the stagnation-point flow problem towards a stretching sheet taking different stretching and straining velocities and they observed two different kinds of boundary layer near the sheet depending on the ratio of the stretching and straining constants. The detailed discussion on the stagnation-point flow over stretching/shrinking sheet can be found in the works of Mahapatra and Gupta [19], Nazar et al. [20], Layek et al. [21], Nadeem et al. [22], Bhattacharyya [23–25], Bhattacharyya et al. [26–28], Bhattacharyya and Vajravelu [29], and Van Gorder et al. [30].

Many fluids used in industries show non-Newtonian behaviour, so the modern-day researchers are more interested in those industrial non-Newtonian fluids and their dynamics. A single constitutive equation is not enough to cover all properties of such non-Newtonian fluids and hence many non-Newtonian fluid models [31–34] have been proposed to clarify all physical behaviours. Casson fluid is one of the

types of such non-Newtonian fluids, which behaves like an elastic solid, and for this fluid, a yield shear stress exists in the constitutive equation. Fredrickson [35] investigated the steady flow of a Casson fluid in a tube. The unsteady boundary layer flow and heat transfer of a Casson fluid over a moving flat plate with a parallel free stream were studied by Mustafa et al. [36] and they solved the problem analytically using homotopy analysis method (HAM). Bhattacharyya et al. [37, 38] reported the exact solution for boundary layer flow of Casson fluid over a permeable stretching/shrinking sheet with and without external magnetic field. The important characteristics of the flows of various non-Newtonian fluids over a stretching/shrinking sheet can be found in the articles [39–46].

Motivated by the previously mentioned investigations on flow of non-Newtonian fluids due to a stretching sheet and its vast applications in many industries, in the present paper, the steady two-dimensional MHD stagnation-point flow of electrically conducting non-Newtonian Casson fluid and heat transfer past a stretching sheet in presence of thermal radiation effect are investigated. Using similarity transformations, the governing equations are transformed. The converted self-similar ordinary differential equations are solved by shooting method. The numerical results are plotted in some figures to see the effects of physical parameters on the flow and heat transfer.

2. Mathematical Analysis of the Flow

Consider the steady two-dimensional incompressible flow of electrically conducting Casson fluid bounded by a stretching sheet at $y = 0$, with the flow being confined in $y > 0$. It is also assumed that the rheological equation of state for an isotropic and incompressible flow of a Casson fluid can be written as [37, 47]

$$\tau_{ij} = \begin{cases} \left(\mu_B + \dfrac{p_y}{\sqrt{2\pi}}\right) 2e_{ij}, & \pi > \pi_c, \\ \left(\mu_B + \dfrac{p_y}{\sqrt{2\pi_c}}\right) 2e_{ij}, & \pi < \pi_c, \end{cases} \tag{1}$$

where μ_B is plastic dynamic viscosity of the non-Newtonian fluid, p_y is the yield stress of fluid, π is the product of the component of deformation rate with itself, namely, $\pi = e_{ij}e_{ij}$, e_{ij} is the (i, j)th component of the deformation rate, and π_c is critical value of π based on non-Newtonian model.

Under the previous conditions, the MHD boundary layer equations for steady stagnation-point flow can be written as

$$\frac{\partial u}{\partial x} + \frac{\partial v}{\partial y} = 0, \tag{2}$$

$$u\frac{\partial u}{\partial x} + v\frac{\partial u}{\partial y} = U_s\frac{dU_s}{dx} + \upsilon\left(1 + \frac{1}{\beta}\right)\frac{\partial^2 u}{\partial y^2} - \frac{\sigma H_0^2}{\rho}\left(u - U_s\right), \tag{3}$$

where u and v are the velocity components in x and y directions, respectively, $U_s = ax$ is the straining velocity of the stagnation-point flow with a (>0) being the straining constant, υ is the kinematic fluid viscosity, ρ is the fluid density, $\beta = \mu_B\sqrt{2\pi_c}/p_y$ is the non-Newtonian or Casson parameter, σ is the electrical conductivity of the fluid, and H_0 is the strength of magnetic field applied in the y direction, with the induced magnetic field being neglected.

The boundary conditions for the velocity components are

$$\begin{aligned} u = U_w, \quad v = 0 \quad \text{at } y = 0, \\ u \longrightarrow U_s \quad \text{as } y \longrightarrow \infty, \end{aligned} \tag{4}$$

where $U_w = cx$ is stretching velocity of the sheet with c (>0) being the stretching constant.

The stream function Ψ is introduced as

$$u = \frac{\partial \Psi}{\partial y}, \qquad v = -\frac{\partial \Psi}{\partial x}. \tag{5}$$

For relations of (5), (2) is satisfied automatically and (3) takes the following form:

$$\begin{aligned} \frac{\partial \Psi}{\partial y}\frac{\partial^2 \Psi}{\partial x \partial y} - \frac{\partial \Psi}{\partial x}\frac{\partial^2 \Psi}{\partial y^2} = U_s\frac{dU_s}{dx} + \upsilon\left(1 + \frac{1}{\beta}\right)\frac{\partial^3 \Psi}{\partial y^3} \\ - \frac{\sigma H_0^2}{\rho}\left(\frac{\partial \Psi}{\partial y} - U_s\right). \end{aligned} \tag{6}$$

Also, boundary conditions in (4) reduce to

$$\begin{aligned} \frac{\partial \Psi}{\partial y} = U_w, \qquad \frac{\partial \Psi}{\partial x} = 0, \quad \text{at } y = 0, \\ \frac{\partial \Psi}{\partial y} \longrightarrow U_s \quad \text{as } y \longrightarrow \infty. \end{aligned} \tag{7}$$

Now, the dimensionless variable for the stream function is implemented as

$$\Psi = \sqrt{c\upsilon}\, x f(\eta), \tag{8}$$

where the similarity variable η is given by $\eta = y\sqrt{c/\upsilon}$.

Using relation (8) and similarity variable, (6) finally takes the following self-similar form:

$$\left(1 + \frac{1}{\beta}\right) f''' + ff'' - f'^2 - M\left(f' - B\right) + B^2 = 0, \tag{9}$$

where primes denote differentiation with respect to η, $M = \sigma H_0^2/\rho c$ is the magnetic parameter, and $B = a/c$ is the velocity ratio parameter.

The boundary conditions reduce to

$$\begin{aligned} f(\eta) = 0, \quad f'(\eta) = 1 \quad \text{at } \eta = 0, \\ f'(\eta) \longrightarrow B \quad \text{as } \eta \longrightarrow \infty. \end{aligned} \tag{10}$$

3. Analysis of Heat Transfer

For the temperature distribution in the flow field with thermal radiation, the governing energy equation can be written as

$$u\frac{\partial T}{\partial x} + v\frac{\partial T}{\partial y} = \frac{\kappa}{\rho c_p}\frac{\partial^2 T}{\partial y^2} - \frac{1}{\rho c_p}\frac{\partial q_r}{\partial y}, \tag{11}$$

where T is the temperature, κ is the thermal conductivity, c_p is the specific heat, and q_r is the radiative heat flux.

The appropriate boundary conditions are

$$\begin{aligned} T &= T_w \quad \text{at } y = 0, \\ T &\longrightarrow T_\infty \quad \text{as } y \longrightarrow \infty, \end{aligned} \tag{12}$$

where T_w is the constant temperature at the sheet and T_∞ is the free stream temperature assumed to be constant.

Using the Rosseland approximation for radiation [48], $q_r = -(4\sigma^*/3k_1)\partial T^4/\partial y$ is obtained, where σ^* is the Stefan-Boltzmann constant and k_1 is the absorption coefficient. We presume that the temperature variation within the flow is such that T^4 may be expanded in a Taylor's series. Expanding T^4 about T_∞ and neglecting higher-order terms we get $T^4 = 4T_\infty^3 T - 3T_\infty^4$.

Now (11) reduces to

$$u\frac{\partial T}{\partial x} + v\frac{\partial T}{\partial y} = \frac{\kappa}{\rho c_p}\frac{\partial^2 T}{\partial y^2} + \frac{16\sigma T_\infty^3}{3k_1\rho c_p}\frac{\partial^2 T}{\partial y^2}. \tag{13}$$

Next, the dimensionless temperature θ is introduced as

$$\theta(\eta) = \frac{T - T_\infty}{T_w - T_\infty}. \tag{14}$$

Using (8), (14), and the similarity variable, (13) reduces to

$$(3R + 4)\theta'' + 3R\mathrm{Pr} f\theta' = 0, \tag{15}$$

where primes denote differentiation with respect to η, $\mathrm{Pr} = c_p\mu/\kappa$ is the Prandtl number, and $R = \kappa^* k_1/4\sigma T_\infty^3$ is the thermal radiation parameter.

The boundary conditions for θ are obtained from (12) as

$$\begin{aligned} \theta(\eta) &= 1 \quad \text{at } \eta = 0, \\ \theta(\eta) &\longrightarrow 0 \quad \text{as } \eta \longrightarrow \infty. \end{aligned} \tag{16}$$

4. Skin Friction Coefficient and Nusselt Number

The physical quantities of interest are the wall skin friction coefficient C_f and the local Nusselt number Nu_x, which are defined as

$$C_f = \frac{\tau_w}{\rho U_w^2(x)}, \qquad \mathrm{Nu}_x = \frac{xq_w}{\alpha(T_w - T_\infty)}, \tag{17}$$

where τ_w is the shear stress or skin friction along the stretching sheet and q_w is the heat flux from the sheet and those are defined as

$$\begin{aligned} \tau_w &= \left(\mu_B + \frac{p_y}{\sqrt{2\pi}}\right)\left(\frac{\partial u}{\partial y}\right)_{y=0}, \\ q_w &= \alpha\left(\frac{\partial T}{\partial y}\right)_{y=0}. \end{aligned} \tag{18}$$

Thus, we get the wall skin friction coefficient C_f and the local Nusselt number Nu_x as follows:

$$\begin{aligned} C_f\sqrt{\mathrm{Re}_x} &= \left(1 + \frac{1}{\beta}\right) f''(0), \\ \frac{\mathrm{Nu}_x}{\sqrt{\mathrm{Re}_x}} &= -\theta'(0), \end{aligned} \tag{19}$$

where $\mathrm{Re}_x = U_w x/\upsilon$ is the local Reynolds number.

5. Numerical Method for Solution

Equations (9) and (15) along with boundary conditions (10) and (16) are solved using shooting method [49–51] by converting them to an initial value problem. In this method, it is necessary to choose a suitable finite value of $\eta \to \infty$, say η_∞. The following system is set

$$\begin{aligned} f' &= p, \qquad p' = q, \\ q' &= \frac{\left\{p^2 + M(p - B) - fq - B^2\right\}}{(1 + 1/\beta)}, \\ \theta' &= z, \qquad z' = \frac{3R\mathrm{Pr} fz}{(3R + 4)} \end{aligned} \tag{20}$$

with the boundary conditions

$$f(0) = 0, \qquad p(0) = 1, \qquad \theta(0) = 1. \tag{21}$$

In order to integrate (20) with (21) as an initial value problem, the values of $q(0)$, that is, $f''(0)$ and $z(0)$, that is, $\theta'(0)$, are required, but no such values are given in the boundary conditions. The suitable guess values for $f''(0)$ and $\theta'(0)$ are chosen and then integration is carried out. Then, the calculated values for f' and θ at $\eta_\infty = 15$ (say) are compared with the given boundary conditions $f'(15) = B$ and $\theta(15) = 0$ and the estimated values, $f''(0)$ and $\theta'(0)$, are adjusted to give a better approximation for the solution. We take the series of values for $f''(0)$ and $\theta'(0)$ and apply the fourth-order classical Runge-Kutta method with step-size $\Delta\eta = 0.01$. The previous procedure is repeated until we get the asymptotically converged results within a tolerance level of 10^{-5}.

6. Results and Discussion

The abovementioned numerical scheme is carried out for various values of physical parameters, namely, the velocity ratio parameter (B), the magnetic parameter (M), the Casson parameter (β), the Prandtl number (Pr), and the thermal radiation parameter (R) to obtain the effects of those parameters on dimensionless velocity and temperature distributions. The obtained computational results are presented graphically in Figures 1–12 and the variations in velocity and temperature are discussed.

Firstly, a comparison of the obtained results with previously published data is performed. The values of wall skin-friction coefficient $f''(0)$ for Newtonian fluid case ($\beta = \infty$)

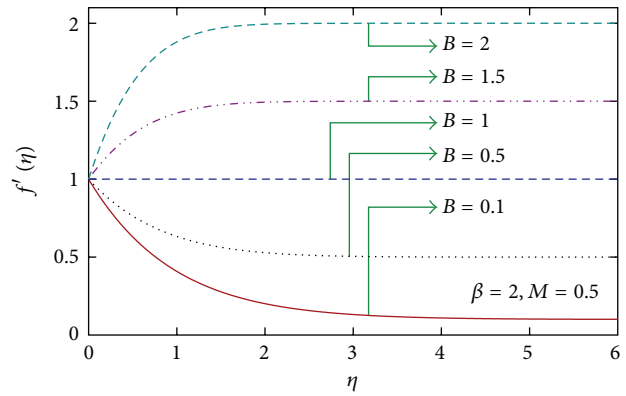

Figure 1: Velocity profiles $f(\eta)$ for several values of B.

Table 1: Values of $f''(0)$ for several values of B with $M = 0$ and $\beta = \infty$ (Newtonian fluid case without magnetic field).

B	Mahapatra and Gupta [19]	Nazar et al. [20]	Present study
0.1	−0.9694	−0.9694	−0.969386
0.2	−0.9181	−0.9181	−0.918107
0.5	−0.6673	−0.6673	−0.667263
2.0	2.0175	2.0176	2.017503
3.0	4.7293	4.7296	4.729284

Table 2: Values of η_δ and $\eta_{\delta T}$ for several values of B, β, M, Pr, and R.

$\beta = 2$, $M = 0.5$, Pr = 1, $R = 1$	$B \rightarrow$		0.1	0.5	1	1.5	2.0
	η_δ		5.76	4.81	—	2.59	2.48
	$\eta_{\delta T}$		10.78	6.59	5.04	4.25	3.75
$M = 0.5$, Pr = 1, $R = 1$	$\beta \rightarrow$		0.5	1	2	5	∞
	η_δ	$B = 0.1$	8.14	6.65	5.76	5.15	4.70
		$B = 2$	3.50	2.86	2.48	2.22	2.03
	$\eta_{\delta T}$	$B = 0.1$	9.45	10.24	10.78	11.17	11.48
		$B = 2$	3.82	3.78	3.75	3.73	3.72
$\beta = 2$, Pr = 1, $R = 1$	$M \rightarrow$		0	0.5	1	2	
	η_δ	$B = 0.1$	6.49	5.76	5.20	4.43	
		$B = 2$	2.53	2.48	2.43	2.33	
	$\eta_{\delta T}$	$B = 0.1$	10.17	10.78	11.21	11.75	
		$B = 2$	3.76	3.75	3.74	3.73	
$\beta = 2$, $M = 0.5$, $R = 1$	Pr $\rightarrow$		0.5	1	2		
	$\eta_{\delta T}$	$B = 0.1$	14.46	10.78	6.69		
		$B = 2$	5.22	3.75	2.70		
$\beta = 2$, $M = 0.5$, Pr = 1	$R \rightarrow$		1	2	5		
	$\eta_{\delta T}$	$B = 0.1$	10.78	8.58	7.09		
		$B = 2$	3.75	3.20	2.81		

in the absence of external magnetic field for different values of velocity ratio parameter (B) are compared with those obtained by Mahapatra and Gupta [19], Nazar et al. [20] in Table 1 in order to verify the validity of the numerical scheme used and those are found in excellent agreement.

The velocity boundary layer thickness (δ) and thermal boundary layer thickness (δ_T) are, respectively, described by the equations $\delta = \eta_\delta \sqrt{\upsilon/c}$ and $\delta_T = \eta_{\delta T}\sqrt{\upsilon/c}$. The dimensionless boundary layer thicknesses η_δ and $\eta_{\delta T}$ are defined as the values of η (nondimensional distance from the surface) at which the difference of dimensionless velocity $f'(\eta)$ and the parameter B has been reduced to 0.001 and the dimensionless temperature $\theta(\eta)$ has been decayed to 0.001, respectively. The velocity and thermal boundary layer thicknesses for various parametric values are given in Table 2. The velocity boundary layer thickness decreases with increasing values B (both for $B > 1$ and $B < 1$) and also the thermal boundary layer thickness decreases with increasing B. So, when the straining velocity rate increases compared to that of stretching velocity rate, then both the boundary layer thicknesses reduce. Actually, downward vorticity due to straining velocity causes the reduction of boundary layer thickness. Similar to velocity ratio parameter, the increase of Casson parameter β also makes the velocity boundary layer thickness thinner. So, the velocity boundary layer thickness for Casson fluid is larger than that of Newtonian fluid. Thus, the plasticity of the fluid causes the increment of the velocity boundary layer thickness. On the other hand, for $B = 0.1$ (<1), the thermal boundary layer thickness increases with increasing values of Casson parameter, but for $B = 2$ (>1) the thermal boundary layer thickness decreases with Casson parameter. Furthermore, due to magnetic field, the velocity boundary layer thickness reduces in all cases. But the thermal boundary layer thickness reduces (increases) for $B = 2$ ($B = 0.1$) with stronger magnetic field. Finally, for the Prandtl number and for radiation parameter, the thermal boundary layer thickness decreases, which is the same as that of Newtonian fluid case.

The velocity and temperature profiles for various values of velocity ratio parameter B are plotted in Figures 1 and 2, respectively. Depending on the velocity ratio parameter, two different kinds of boundary layers are obtained as described by Mahapatra and Gupta [18] for Newtonian fluid. In the first kind, the velocity of fluid inside the boundary layer decreases from the surface towards the edge of the layer (for $B < 1$) and in the second kind the fluid velocity increases from the surface towards the edge (for $B > 1$). Those characters can be seen from velocity profiles in Figure 1. Also, it is important to note that if $B = 1$ ($a = c$), that is, the stretching velocity and the straining velocity are equal, then there is no boundary layer of Casson fluid flow near the sheet, which is similar to that of Chiam's [17] observation for Newtonian fluid. From Figure 2, it is seen that in all cases thermal boundary layer is formed and the temperature at a point decreases with B.

The effects of Casson parameter β on the velocity and temperature fields are depicted in Figures 3 and 4. It is worthwhile to note that the velocity increases with the increase in values of β for $B = 2$ and it decreases with β for $B = 0.1$. Consequently, the velocity boundary layer thickness reduces for both values of B. Due to the increase of Casson parameter β, the yield stress p_y falls and consequently

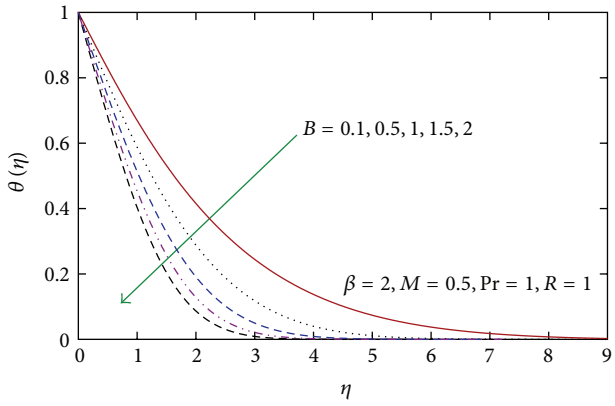

FIGURE 2: Temperature profiles $\theta(\eta)$ for several values of B.

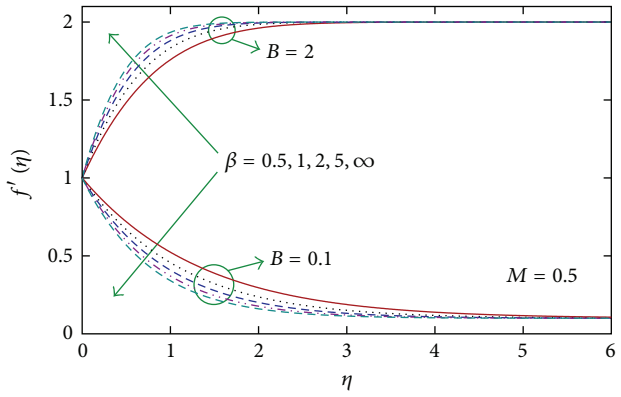

FIGURE 3: Velocity profiles $f(\eta)$ for several values of β.

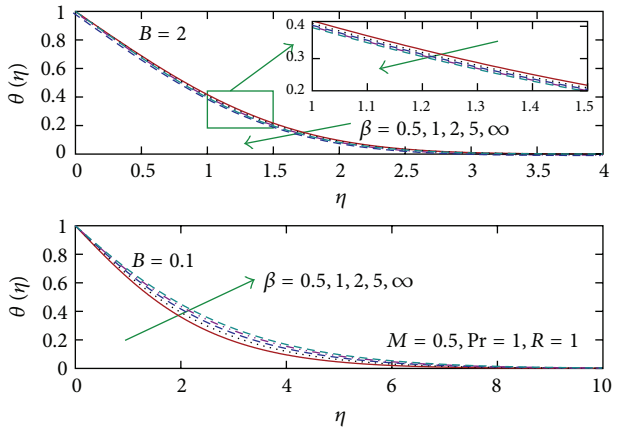

FIGURE 4: Temperature profiles $\theta(\eta)$ for several values of β.

velocity boundary layer thickness decreases. The influences of Casson parameter on the temperature profiles are different in two cases, $B = 2$ and $B = 0.1$. Temperature at a point decreases with increasing β for $B = 2$ and increases with increasing β for $B = 0.1$.

In Figures 5 and 6, the velocity and temperature profiles are presented for several values of magnetic parameter M. Similar to that of Casson parameter, due to the increase of

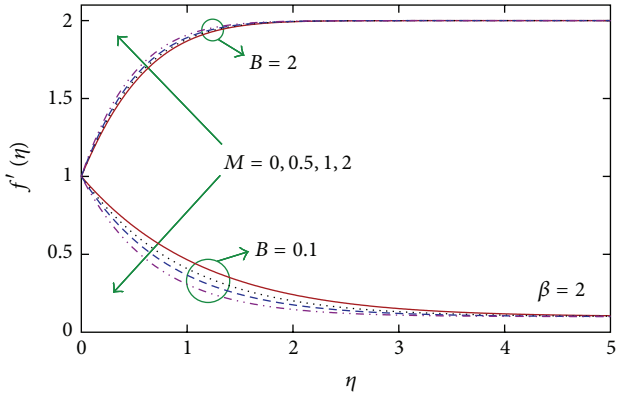

FIGURE 5: Velocity profiles $f(\eta)$ for several values of M.

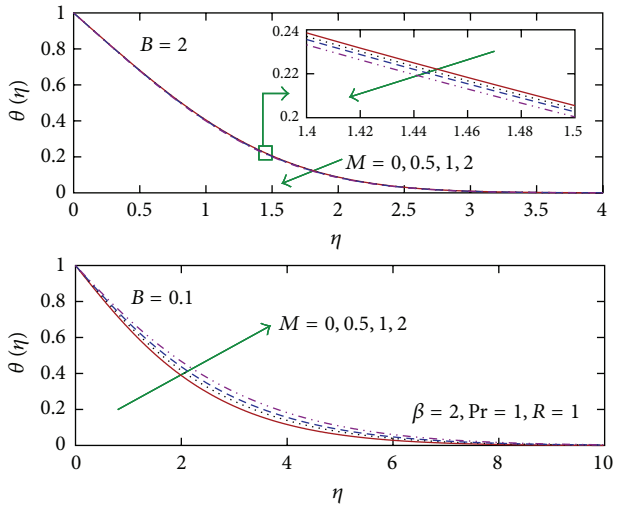

FIGURE 6: Temperature profiles $\theta(\eta)$ for several values of M.

magnetic parameter the dimensionless velocity at fixed η increases for $B = 2$ and for $B = 0.1$ the velocity decreases. Consequently, for both types of boundary layers, the thickness decreases. The Lorentz force induced by the dual actions of electric and magnetic fields reduces the velocity boundary layer thickness by opposing the transport phenomenon. Also, for $B = 2$, the temperature decreases with M and increases with M for $B = 0.1$.

The dimensionless temperature profiles $\theta(\eta)$ for several values of Prandtl Number Pr and thermal radiation parameter R are exhibited in Figures 7 and 8, respectively, for two values of B. In both cases ($B = 0.1$ and 2), the temperature decreases with increasing values of Prandtl number and radiation parameter and the thermal boundary layer thickness becomes smaller in all cases. Actually, the rate of heat transfer is enhanced with Prandtl Number and radiation parameter and this causes the reduction of thermal boundary layer thickness.

The physical quantities, the wall skin friction coefficient C_f, and the local Nusselt number Nu_x, which have immense engineering applications, are proportional to the values of $(1 + 1/\beta)f''(0)$ and $-\theta'(0)$, respectively. The values of $(1 +$

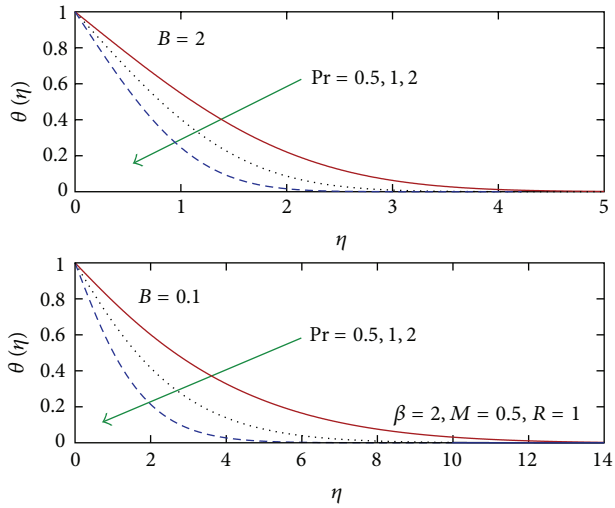

FIGURE 7: Temperature profiles $\theta(\eta)$ for several values of Pr.

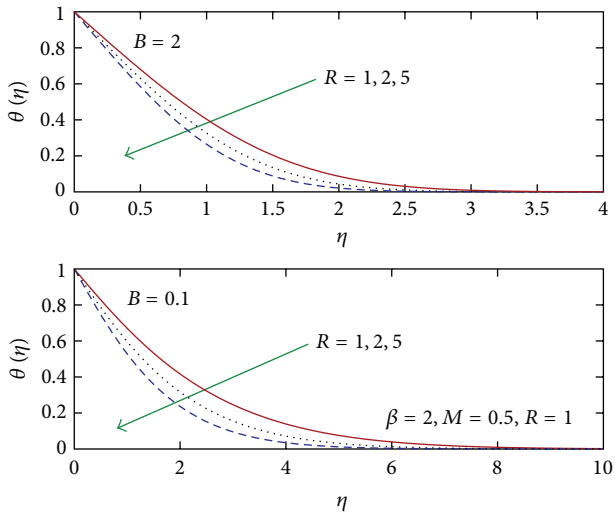

FIGURE 8: Temperature profiles $\theta(\eta)$ for several values of R.

$1/\beta) f''(0)$ and $-\theta'(0)$ against the magnetic parameter M are plotted in Figures 9 and 10 for different values of B. From the figures, it is observed that the magnitude of wall skin friction coefficient decreases with increasing values of velocity ratio parameter B when $B < 0.1$, whereas for $B > 0.1$ the magnitude of skin-friction increases with B. The local Nusselt number (Figure 10) increases with B; that is, the heat transfer rate is enhanced with B. Due to higher values of Casson parameter β, the magnitude of $(1 + 1/\beta) f''(0)$ decreases (Figure 11) for both values of B (for $B > 1$ as well as for $B < 1$). On the other hand, the value of $-\theta'(0)$, that is, the heat transfer (Figure 12), increases with β for $B = 2$ (>1) and decreases with β when $B = 0.1$ (<1). Finally, from those figures (Figures 9–12), it can be noticed that the wall skin friction coefficient always becomes larger when the external magnetic field is stronger and the rate of heat transfer is enhanced (reduced) with increasing magnetic parameter M for $B > 1$ ($B < 1$).

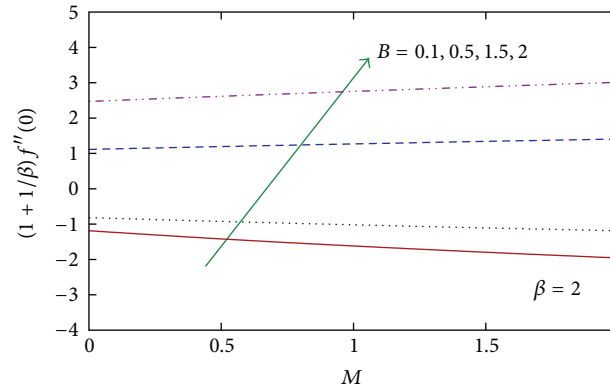

FIGURE 9: The values of $(1+1/\beta) f''(0)$ for several values of B and M.

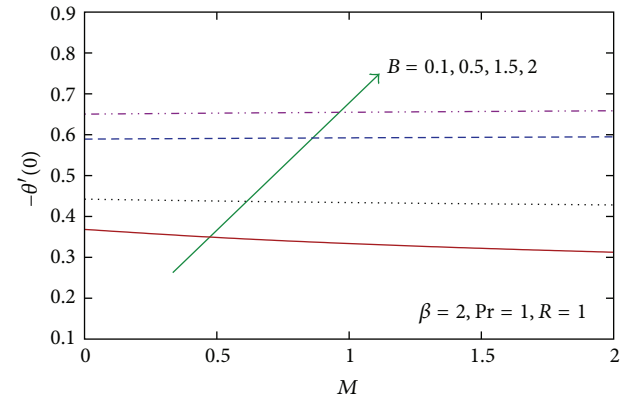

FIGURE 10: The values of $-\theta'(0)$ for several values of B and M.

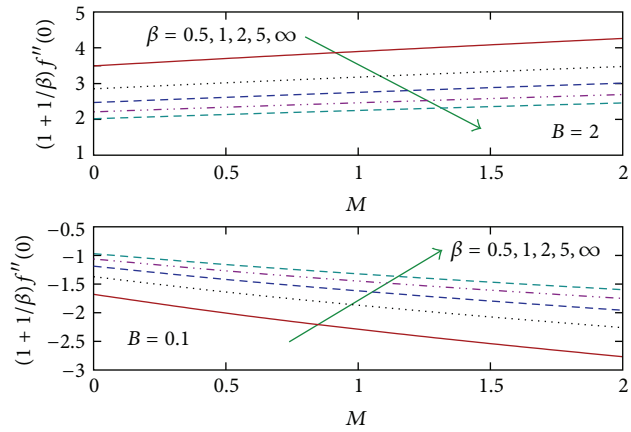

FIGURE 11: The values of $(1 + 1/\beta) f''(0)$ for several values of β and M.

7. Conclusions

The MHD stagnation-point flow of Casson fluid and heat transfer over a stretching sheet are investigated taking into consideration the thermal radiation effect. Using similarity transformations, the governing equations are transformed to self-similar ordinary differential equations which are then

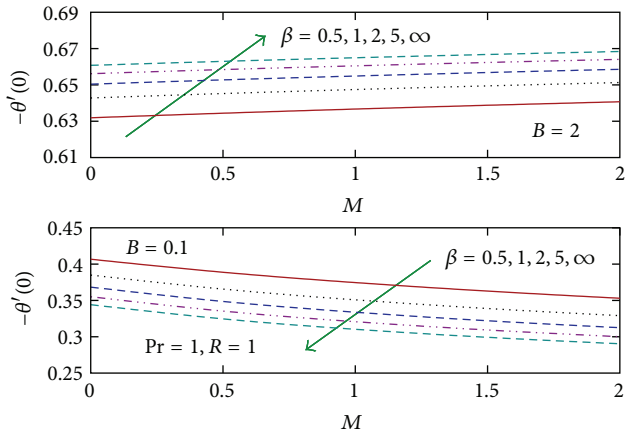

FIGURE 12: The values of $-\theta'(0)$ for several values of β and M.

solved using shooting method. From the study, the following remarks can be summarized.

(a) The velocity boundary layer thickness reduces with velocity ratio parameter and magnetic parameter.

(b) The velocity boundary layer thickness for Casson fluid is larger than that of Newtonian fluid.

(c) For Casson fluid, that is, for decrease of Casson parameter, the thermal boundary layer thickness decreases for $B = 0.1$ (<1) and, in contrast, for $B = 2$ (>1) the thickness increases.

(d) Due to thermal radiation, the temperature inside the boundary layer decreases.

(e) The magnitude of wall skin-friction coefficient decreases with Casson parameter β.

Nomenclature

a: Straining constant
B: Velocity ratio parameter
c: Stretching constant
C_f: Wall skin friction coefficient
c_p: Specific heat
f: Dimensionless stream function
f': Dimensionless velocity
H_0: Strength of magnetic field applied in the y direction
k_1: Absorption coefficient
M: Magnetic parameter
Nu_x: Local Nusselt number
Pr: Prandtl number
p: A variable
p_y: Yield stress of fluid
q: A variable
q_r: Radiative heat flux
q_w: Heat flux from the sheet
R: Thermal radiation parameter
Re_x: Local Reynolds number
T: Temperature
T_w: Constant temperature at the sheet
T_∞: Free stream temperature
U_s: Straining velocity of the stagnation-point flow
U_w: Stretching velocity of the sheet
u: Velocity component in x direction
v: Velocity component in y direction
x: Distance along the sheet
y: Distance perpendicular to the sheet
z: A variable.

Greek Symbols

β: Non-Newtonian/Casson parameter
δ: Velocity boundary layer thickness
δ_T: Thermal boundary layer thickness
η: Similarity variable
η_∞: Finite value of η
η_δ: Dimensionless velocity boundary layer thickness
$\eta_{\delta T}$: Dimensionless thermal boundary layer thickness
κ: Thermal conductivity
μ_B: Plastic dynamic viscosity of the non-Newtonian fluid
π: Product of the component of deformation rate with itself
π_c: Critical value of π
υ: Kinematic fluid viscosity
ρ: Fluid density
Ψ: Stream function
σ: Electrical conductivity of the fluid
σ^*: Stefan-Boltzmann constant
τ_w: Shear stress
θ: Dimensionless temperature.

Conflict of Interests

The author declares that there is no conflict of interests regarding the publication of this paper.

Acknowledgments

The author gratefully acknowledges the financial support of the *National Board for Higher Mathematics* (NBHM), Department of Atomic Energy, Government of India, for pursuing this work. The author also thanks the referees for their valuable comments and suggestions which helped a lot in the improvement of the quality of the paper.

References

[1] L. J. Crane, "Flow past a stretching plate," *Zeitschrift für Angewandte Mathematik und Physik*, vol. 21, no. 4, pp. 645–647, 1970.

[2] K. B. Pavlov, "Magnetohydrodynamic flow of an incompressible viscous fluid caused by the deformation of a plane surface," *Magnetohydrodynamics*, vol. 10, pp. 146–148, 1974.

[3] H. I. Andersson, "MHD flow of a viscoelastic fluid past a stretching surface," *Acta Mechanica*, vol. 95, no. 1–4, pp. 227–230, 1992.

[4] S. Mukhopadhyay, G. C. Layek, and S. A. Samad, "Study of MHD boundary layer flow over a heated stretching sheet with variable viscosity," *International Journal of Heat and Mass Transfer*, vol. 48, no. 21-22, pp. 4460–4466, 2005.

[5] T. Fang and J. Zhang, "Closed-form exact solutions of MHD viscous flow over a shrinking sheet," *Communications in Nonlinear Science and Numerical Simulation*, vol. 14, no. 7, pp. 2853–2857, 2009.

[6] K. Bhattacharyya and G. C. Layek, "Chemically reactive solute distribution in MHD boundary layer flow over a permeable stretching sheet with suction or blowing," *Chemical Engineering Communications*, vol. 197, no. 12, pp. 1527–1540, 2010.

[7] K. Bhattacharyya, "Effects of radiation and heat source/sink on unsteady MHD boundary layer flow and heat transfer over a shrinking sheet with suction/injection," *Frontiers of Chemical Engineering in China*, vol. 5, no. 3, pp. 376–384, 2011.

[8] K. Bhattacharyya, "Effects of heat source/sink on mhd flow and heat transfer over a shrinking sheet with mass suction," *Chemical Engineering Research Bulletin*, vol. 15, no. 1, pp. 12–17, 2011.

[9] K. Bhattacharyya and I. Pop, "MHD Boundary layer flow due to an exponentially shrinking sheet," *Magnetohydrodynamics*, vol. 47, pp. 337–344, 2011.

[10] H. Tabaei, M. A. Moghimi, A. Kimiaeifar, and M. A. Moghimi, "Homotopy analysis and differential quadrature solution of the problem of free-convective magnetohydrodynamic flow over a stretching sheet with the Hall effect and mass transfer taken into account," *Journal of Applied Mechanics and Technical Physics*, vol. 52, no. 4, pp. 624–636, 2011.

[11] R. Kandasamy, I. Muhaimin, and G. Kamachi, "Scaling group transformation for the effect of temperature-dependent nanofluid viscosity on an mhd boundary layer past a porous stretching surface," *Journal of Applied Mechanics and Technical Physics*, vol. 52, no. 6, pp. 931–940, 2011.

[12] A. M. Salem and R. Fathy, "Effects of variable properties on MHD heat and mass transfer flow near a stagnation point towards a stretching sheet in a porous medium with thermal radiation," *Chinese Physics B*, vol. 21, Article ID 054701, 2012.

[13] S. Mukhopadhyay and R. S. R. Gorla, "Effects of partial slip on boundary layer flow past a permeable exponential stretching sheet in presence of thermal radiation," *Heat and Mass Transfer*, vol. 48, pp. 1773–1781, 2012.

[14] K. Bhattacharyya and G. C. Layek, "Slip effect on diffusion of chemically reactive species in boundary layer flow over a vertical stretching sheet with suction or blowing," *Chemical Engineering Communications*, vol. 198, no. 11, pp. 1354–1365, 2011.

[15] K. Bhattacharyya, "Boundary layer flow and heat transfer over an exponentially shrinking sheet," *Chinese Physics Letters*, vol. 28, no. 7, Article ID 074701, 2011.

[16] I. C. Mandal and S. Mukhopadhyay, "Heat transfer analysis for fluid flow over an exponentially stretching porous sheet with surface heat flux in porous medium," *Ain Shams Engineering Journal*, vol. 4, pp. 103–110, 2013.

[17] T. C. Chiam, "Stagnation-point flow towards a stretching plate," *Journal of the Physical Society of Japan*, vol. 63, no. 6, pp. 2443–2444, 1994.

[18] T. R. Mahapatra and A. S. Gupta, "Magnetohydrodynamic stagnation-point flow towards a stretching sheet," *Acta Mechanica*, vol. 152, no. 1-4, pp. 191–196, 2001.

[19] T. R. Mahapatra and A. S. Gupta, "Heat transfer in stagnation-point flow towards a stretching sheet," *Heat and Mass Transfer*, vol. 38, no. 6, pp. 517–521, 2002.

[20] R. Nazar, N. Amin, D. Filip, and I. Pop, "Unsteady boundary layer flow in the region of the stagnation point on a stretching sheet," *International Journal of Engineering Science*, vol. 42, no. 11-12, pp. 1241–1253, 2004.

[21] G. C. Layek, S. Mukhopadhyay, and S. A. Samad, "Heat and mass transfer analysis for boundary layer stagnation-point flow towards a heated porous stretching sheet with heat absorption/generation and suction/blowing," *International Communications in Heat and Mass Transfer*, vol. 34, no. 3, pp. 347–356, 2007.

[22] S. Nadeem, A. Hussain, and M. Khan, "HAM solutions for boundary layer flow in the region of the stagnation point towards a stretching sheet," *Communications in Nonlinear Science and Numerical Simulation*, vol. 15, no. 3, pp. 475–481, 2010.

[23] K. Bhattacharyya, "Dual solutions in boundary layer stagnation-point flow and mass transfer with chemical reaction past a stretching/shrinking sheet," *International Communications in Heat and Mass Transfer*, vol. 38, no. 7, pp. 917–922, 2011.

[24] K. Bhattacharyya, "Dual solutions in unsteady stagnation-point flow over a shrinking sheet," *Chinese Physics Letters*, vol. 28, no. 8, Article ID 084702, 2011.

[25] K. Bhattacharyya, "Heat transfer in unsteady boundary layer stagnation-point flow towards a shrinking sheet," *Ain Shams Engineering Journal*, vol. 4, pp. 259–264, 2013.

[26] K. Bhattacharyya, S. Mukhopadhyay, and G. C. Layek, "Reactive solute transfer in magnetohydrodynamic boundary layer stagnation-point flow over a stretching sheet with suction/blowing," *Chemical Engineering Communications*, vol. 199, no. 3, pp. 368–383, 2012.

[27] K. Bhattacharyya, M. G. Arif, and W. A. Pramanik, "MHD boundary layer stagnation-point flow and mass transfer over a permeable shrinking sheet with suction/blowing and chemical reaction," *Acta Technica*, vol. 57, pp. 1–15, 2012.

[28] K. Bhattacharyya, S. Mukhopadhyay, and G. C. Layek, "Slip effects on an unsteady boundary layer stagnation-point flow and heat transfer towards a stretching sheet," *Chinese Physics Letters*, vol. 28, no. 9, Article ID 094702, 2011.

[29] K. Bhattacharyya and K. Vajravelu, "Stagnation-point flow and heat transfer over an exponentially shrinking sheet," *Communications in Nonlinear Science and Numerical Simulation*, vol. 17, no. 7, pp. 2728–2734, 2012.

[30] R. A. Van Gorder, K. Vajravelu, and I. Pop, "Hydromagnetic stagnation point flow of a viscous fluid over a stretching or shrinking sheet," *Meccanica*, vol. 47, no. 1, pp. 31–50, 2012.

[31] W. L. Wilkinson, "The drainage of a maxwell liquid down a vertical plate," *The Chemical Engineering Journal*, vol. 1, no. 3, pp. 255–257, 1970.

[32] K. R. Rajagopal, "Viscometric flows of third grade fluids," *Mechanics Research Communications*, vol. 7, no. 1, pp. 21–25, 1980.

[33] K. R. Rajagopal, T. Y. Na, and A. S. Gupta, "Flow of a viscoelastic fluid over a stretching sheet," *Rheologica Acta*, vol. 23, no. 2, pp. 213–215, 1984.

[34] C. Dorier and J. Tichy, "Behavior of a bingham-like viscous fluid in lubrication flows," *Journal of Non-Newtonian Fluid Mechanics*, vol. 45, no. 3, pp. 291–310, 1992.

[35] A. G. Fredrickson, *Principles and Applications of Rheology*, Prentice-Hall, Englewood Cliffs, NJ, USA, 1964.

[36] M. Mustafa, T. Hayat, I. Pop, and A. Aziz, "Unsteady boundary layer flow of a Casson fluid due to an impulsively started moving flat plate," *Heat Transfer*, vol. 40, no. 6, pp. 563–576, 2011.

[37] K. Bhattacharyya, T. Hayat, and A. Alsaedi, "Exact solution for boundary layer flow of Casson fluid over a permeable stretching/shrinking sheet," *Zeitschrift für Angewandte Mathematik und Mechanik*, 2013.

[38] K. Bhattacharyya, T. Hayat, and A. Alsaedi, "Analytic solution for magnetohydrodynamic boundary layer flow of Casson fluid over a stretching/shrinking sheet with wall mass transfer," *Chinese Physics B*, vol. 22, Article ID 024702, 2013.

[39] T. Hayat, Z. Abbas, and N. Ali, "MHD flow and mass transfer of a upper-convected Maxwell fluid past a porous shrinking sheet with chemical reaction species," *Physics Letters Section A*, vol. 372, no. 26, pp. 4698–4704, 2008.

[40] T. Hayat, S. Iram, T. Javed, and S. Asghar, "Shrinking flow of second grade fluid in a rotating frame: an analytic solution," *Communications in Nonlinear Science and Numerical Simulation*, vol. 15, no. 10, pp. 2932–2941, 2010.

[41] K.-L. Hsiao, "Viscoelastic fluid over a stretching sheet with electromagnetic effects and nonuniform heat source/sink," *Mathematical Problems in Engineering*, vol. 2010, Article ID 740943, 14 pages, 2010.

[42] B. Sahoo and S. Poncet, "Flow and heat transfer of a third grade fluid past an exponentially stretching sheet with partial slip boundary condition," *International Journal of Heat and Mass Transfer*, vol. 54, no. 23-24, pp. 5010–5019, 2011.

[43] K. Bhattacharyya, S. Mukhopadhyay, G. C. Layek, and I. Pop, "Effects of thermal radiation on micropolar fluid flow and heat transfer over a porous shrinking sheet," *International Journal of Heat and Mass Transfer*, vol. 55, no. 11-12, pp. 2945–2952, 2012.

[44] S. Mukhopadhyay, "Casson fluid flow and heat transfer over a nonlinearly stretching," *Chinese Physics B*, vol. 22, Article ID 074701, 2013.

[45] S. Mukhopadhyay, P. R. De, and G. C. Layek, "Heat transfer characteristics for the Maxwell fluid flow past an unsteady stretching permeable surface embedded in a porous medium with thermal radiation," *Journal of Applied Mechanics and Technical Physics*, vol. 54, pp. 385–396, 2013.

[46] T. Javed, N. Ali, Z. Abbas, and M. Sajid, "Flow of an Eyring-Powell non-Newtonian fluid over a stretching sheet," *Chemical Engineering Communications*, vol. 200, pp. 327–336, 2013.

[47] M. Nakamura and T. Sawada, "Numerical study on the flow of a non-Newtonian fluid through an axisymmetric stenosis," *Journal of Biomechanical Engineering*, vol. 110, no. 2, pp. 137–143, 1988.

[48] M. Q. Brewster, *Thermal Radiative Transfer Properties*, John Wiley and Sons, 1972.

[49] K. Bhattacharyya, S. Mukhopadhyay, and G. C. Layek, "MHD boundary layer slip flow and heat transfer over a flat plate," *Chinese Physics Letters*, vol. 28, no. 2, Article ID 024701, 2011.

[50] S. Mukhopadhyay, K. Bhattacharyya, and G. C. Layek, "Steady boundary layer flow and heat transfer over a porous moving plate in presence of thermal radiation," *International Journal of Heat and Mass Transfer*, vol. 54, no. 13-14, pp. 2751–2757, 2011.

[51] K. Bhattacharyya, "Dual solutions in boundary layer stagnation-point flow and mass transfer with chemical reaction past a stretching/shrinking sheet," *International Communications in Heat and Mass Transfer*, vol. 38, no. 7, pp. 917–922, 2011.

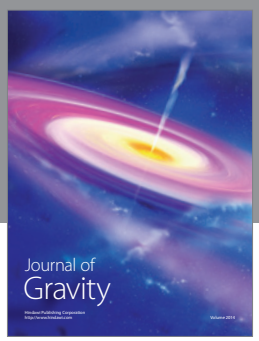

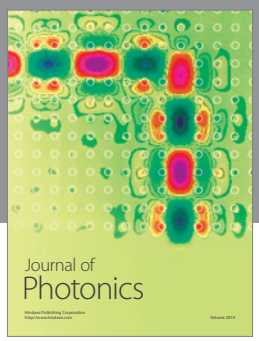

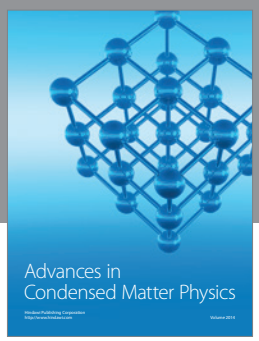

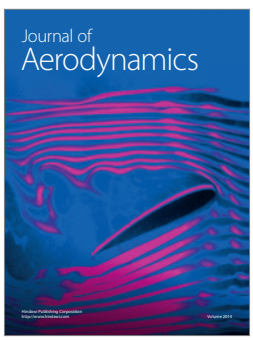

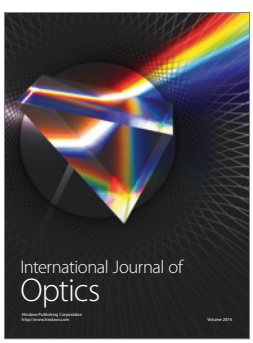

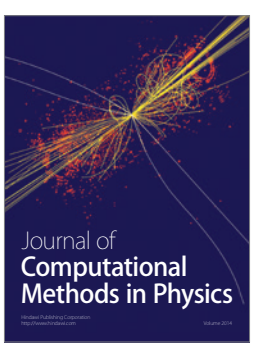

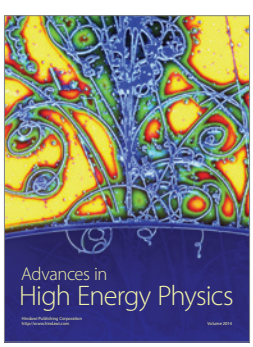

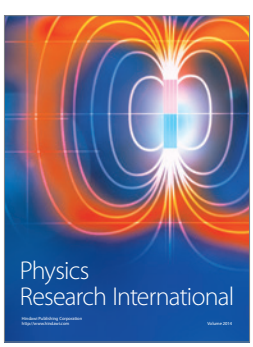

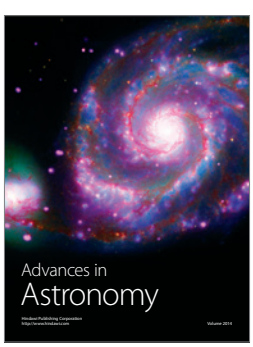

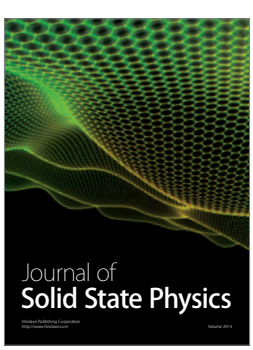

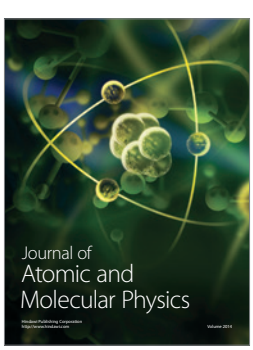

Hindawi

Submit your manuscripts at
http://www.hindawi.com